Mitochondrial volume fraction controls translation of nuclear-encoded mitochondrial proteins

Tatsuhisa Tsuboi[1,2,✉], Matheus P. Viana[2,7], Fan Xu[1], Jingwen Yu[1], Raghav Chanchani[1], Ximena G. Arceo[1], Evelina Tutucci[3], Joonhyuk Choi[1], Yang S. Chen[1], Robert H. Singer[3,4,5,6], Susanne M. Rafelski[2,7,✉], and Brian M. Zid[1,✉]

[1]Department of Chemistry and Biochemistry, University of California San Diego, La Jolla, San Diego, CA 92023, USA
[2]Department of Developmental and Cell Biology, University of California Irvine, Irvine, CA 92697-2300, USA
[3]Department of Anatomy and Structural Biology, Albert Einstein College of Medicine, Bronx, NY 10461, USA
[4]Gruss-Lipper Biophotonics Center, Albert Einstein College of Medicine, Bronx, NY 10461, USA
[5]Department of Neuroscience, Albert Einstein College of Medicine, Bronx, NY 10461, USA
[6]Janelia Research Campus, Howard Hughes Medical Institute (HHMI), Ashburn, VA 20147, USA
[7]Currently at Allen Institute for Cell Science, Seattle, WA 98109, USA

Mitochondria are dynamic in their size and morphology yet must also precisely control their protein composition according to cellular energy demand. This control is particularly complicated for mitochondria, as they must coordinate gene expression from both the nuclear and mitochondrial genome. We have found that cells are able to use this dynamic morphology to post-transcriptionally coordinate protein expression with the metabolic demands of the cell through enhanced mRNA localization to the mitochondria. As yeast switch to respiratory metabolism, they increase their mitochondrial volume fraction - that is, the ratio of mitochondrial volume to intracellular volume - which drives the localization of nuclear-encoded mitochondrial mRNAs to the surface of the mitochondria. Through artificial tethering experiments, we show that this mitochondrial localization is sufficient to increase protein production, whereas sequestering mRNAs away from the mitochondrial surface decreases protein production, and those cells are deficient in growth in respiratory conditions. Furthermore, we find that this mRNA sensitivity to mitochondrial volume fraction is driven by the speed of translation downstream of the mitochondrial targeting sequence (MTS), as local ribosome stalling through a stretch of polyprolines in the nascent peptide can drive constitutive localization of mRNAs to the mitochondria. This points to a mechanism by which organelle volume fraction provides feedback to regulate organelle-specific gene expression through mRNA localization while potentially circumventing the need to directly coordinate with the nuclear genome.

mitochondria | geometric constraints | mRNA localization | translation control

Correspondence: ***ttsuboi@ucsd.edu, susanner@uci.edu, zid@ucsd.edu***

Oxidative phosphorylation protein coding mRNAs are known to gradually increase their protein synthesis as the growth environment changes from vegetative growth (glucose) to respiratory conditions (glycerol) (1). mRNAs for many nuclear-encoded mitochondrial proteins are localized and even translated on the surface of the mitochondria. We sought to explore this mRNA localization under different metabolic states to further understand how it is controlled as well as its potential impact on mitochondrial protein synthesis. To analyze the relationship between mitochondria and mRNA localization in live cells, we visualized mitochondria using the matrix marker Su9-mCherry and single molecule mRNA by the MS2-MCP system every 3 seconds in a microfluidic device (Fig. 1A, Extended Data Fig. 1, and Methods). We first analyzed three different mRNAs. Two mRNAs have previously been seen to be mitochondrially localized and contain an MTS: *ATP3* mRNA, which encodes the gamma subunit of ATP synthase, and *TIM50*, which encodes a component of the inner membrane translocase. The third mRNA, *TOM22*, encodes an outer membrane translocase that does not contain an MTS and has previously been found to be predominantly diffusely localized (2–4). During vegetative growth, we observed *TIM50* mRNA to be strongly associated with the mitochondria, while *TOM22* showed low association (Fig. 1B, Extended Data Fig. 2, and Methods). Even though *ATP3* had previously been categorized as a mitochondrially localized mRNA (4), we unexpectedly found this to be condition dependent, as it has low association with mitochondria, similar to *TOM22*, in vegetative conditions. However, during respiratory conditions it strongly shifted towards association with the mitochondrial surface, in a manner more similar to *TIM50* (Fig. 1B). This means that nuclear-encoded mitochondrial mRNAs do not have to be solely mitochondrially localized or diffusely localized; instead, they can show a switch-like behavior depending on the metabolic needs of the cell.

As yeast cells shift to respiratory conditions, the mitochondrial volume increases while the cell cytoplasmic volume decreases, thus leading to an increase in the mitochondrial volume fraction in respiratory conditions (Fig. 1C, Extended Data Fig. 3) (5). While *ATP3* mRNA showed a strong condition dependent localization, *TIM50* and *TOM22* mRNAs also showed modestly increased mitochondrial association during respiratory conditions. (Fig. 1B). We wondered what impact the reduction in the availability of free cytoplasmic space due to mitochondrial expansion had on mRNA co-localization, especially for *TOM22*, which is not known to bind the mitochondria. To test this, we quantified the mitochondrial localization of each mRNA while also quantifying the changing mitochondrial volume fraction at a single-cell

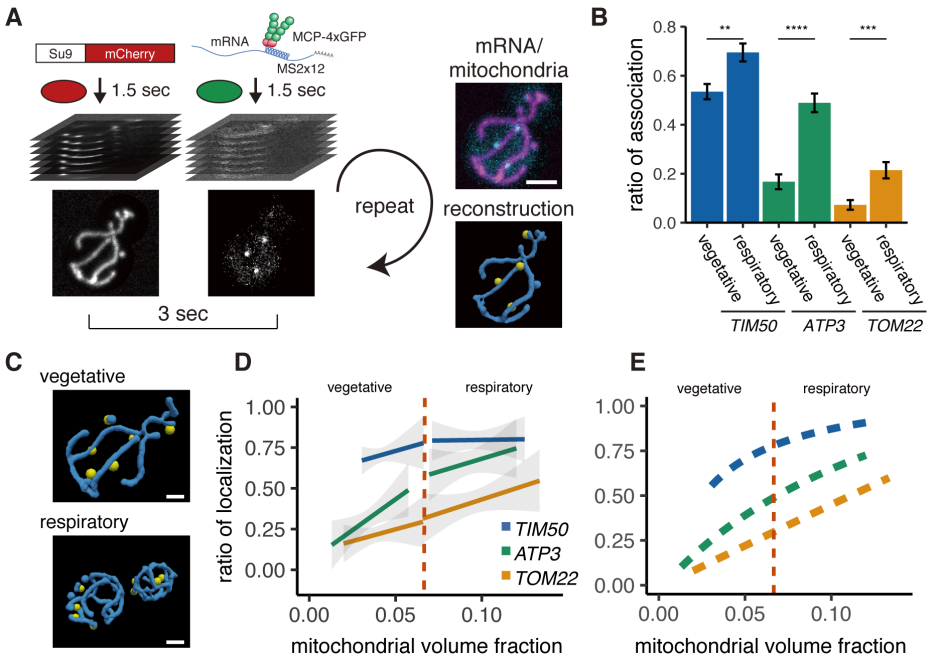

Fig. 1. Mitochondrial volume fraction correlates with mRNA localization. (A) Experimental setup for live imaging. Mitochondria were visualized by Su9-mCherry and mRNAs were visualized by the single molecule MS2-MCP tethering system. Z-stacks were taken within 1.5 sec for each individual channel and multiple Z-stacks were merged into a series. (Right top) Z-projected image of a live cell. Cyan: mRNA, Purple: matrix (Right bot) Reconstructed mRNA and mitochondria, Yellow: mRNA, Blue: mitochondria. Scale bar, 2 µm. (B) The ratio of the mitochondrial associated mRNA per cell (n>27) of the different mRNA species in vegetative and respiratory conditions. Error bar represents standard error of the mean (s.e.m.). Statistical significance was assessed by Mann–Whitney U-test (**** P < 0.0001; *** P < 0.001; ** P < 0.01). (C) Snapshot of reconstructed mitochondrial surface (blue) and *TIM50* mRNA foci (yellow) in vegetative and respiratory conditions. Scale bar, 1 µm. (D) Relationship between the mitochondrial volume fraction and the ratio of mRNA localization to mitochondria. Trend line was depicted according to the best linear fit of the ratio of localization and mitochondrial volume fraction of single cells in each condition of different mRNAs (n>27). Dotted red line marks the difference between vegetative and respiratory conditions for mitochondria volume fraction. Gray region surrounding the trend lines represents the 95 confidence interval (CI) for each line. (E) Mitochondrial volume fraction and mRNA localization have stoichiometric correlation. Relationship of ratio of mRNA localization to mitochondria and mitochondrial volume fraction from mathematical modeling was plotted. Yellow line represents linearly fitted line for *TOM22* mRNA. Green and blue lines were plotted through equilibrium constant of $2.4K_0$ and $8.8K_0$, respectively as described in Methods.

level. We found that *TOM22* showed a linear increase in co-localization that was directly proportional to mitochondrial volume fraction (Fig. 1D). Surprisingly, we found that *ATP3* mRNA was more sensitive to mitochondrial volume fraction than *TIM50* and *TOM22*. This sensitivity was independent of nutrients, as vegetative yeast cells also showed a larger increase in *ATP3* localization as the mitochondrial volume fraction increased (Fig. 1D). At the lowest mitochondrial volume fractions *ATP3* localization was similar to the unlocalized *TOM22* mRNA, while at the highest volume fractions its localization was close to the mitochondrially localized mRNA *TIM50*. This suggests that increased mitochondrial volume fraction drives *ATP3* mRNA localization to mitochondria.

To gain more insight into how mitochondrial volume fraction is affecting mRNA localization, we designed in silico experiments based on our experimentally measured cell and mitochondrial boundaries and mathematically modeled how particles of varying affinities would co-localize with the mitochondria. We were able to recapitulate the behaviour of *TOM22* by simply modeling an ideal Brownian particle with no affinity for the mitochondria, which showed linearly-correlated localization with mitochondrial volume fraction. We then set up a simple equilibrium equation where the baseline equilibrium constant, K_0, was set by a freely diffusing particle like *TOM22* and multiplied by the affinity, A, of the particle for the mitochondria thus giving $K = AK_0$ (Methods). As the value of A increased in the simulation, the ratio of mitochondrial localization of the mRNA for a given mitochondrial volume fraction increased as well (Fig. 1F). We then applied this relationship to estimate the experimental values of A to be 2.4 and 8.8 for *ATP3* and *TIM50*, respectively (Fig. 1E). Interestingly, this simple mathematical relationship also recapitulates the shape of the curves in Figure 1D, suggesting that the apparent shift in association occurring during the switch from vegetative to respiratory conditions may be solely a result of the combination of the mitochondrial volume fraction and the strength of mRNA sequence-specific association and therefore not due to the difference in growth condition or to other mechanisms. The association between an mRNA and mitochondria can thus be tuned to permit a switch-like transition in mitochondrial localization purely due to a nutrient-induced change in mitochondrial volume fraction independent of any other regulation, as is seen for *ATP3* mRNA (Fig. 1B).

To further analyze the functional role for this varied increase in mRNA localization, we compared mRNA levels (via number of mRNAs per single cell) with protein levels (via both single cell measurements and bulk assays) in both vegetative and respiratory conditions. Atp3 protein levels increased four-fold while mRNA levels increased less than two-fold when cells were grown in vegetative versus respiratory conditions. *TIM50* mRNA, which is constitutively local-

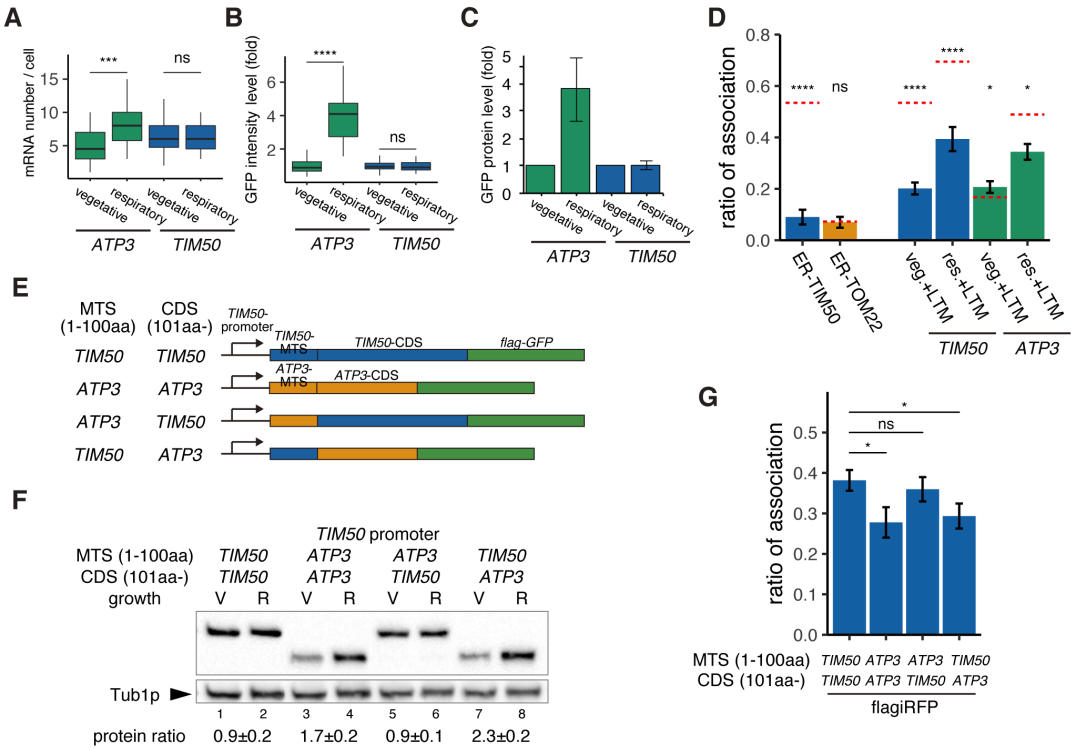

Fig. 2. Increased protein synthesis and mRNA localization is regulated by the downstream coding sequence. (A) *ATP3* mRNA and *TIM50* mRNA expression number per cell. MCP-GFP foci were counted per cell (n>27). (B) Atp3p-GFP and Tim50p-GFP fusion protein expression level using GFP fluorescent intensity per cell. Statistical significance was assessed by Mann–Whitney U-test (**** P < 0.0001; *** P < 0.001; ns, no significant difference). (C) Atp3p-GFP and Tim50p-GFP fusion protein expression level using western blotting with anti-GFP antibody. Error indicates standard deviation of three independent experiments. (D) ER-localization signal and translational inhibitor drugs alter the ratio of the mitochondrial associated mRNA per cell of the strains in Fig. 1B (n>20). LTM, 50μM for 20min. Error bar represents s.e.m. Statistical significance compared with control (value in Fig. 1B, red dotted line) was assessed by Mann–Whitney U-test (**** P < 0.0001; * P < 0.05; ns, no significant difference). (E) Schematic of chimeric reporter genes for swapping of MTS (1-100aa) and CDS (101aa-) between *TIM50* and *ATP3*. (F) Protein expression from reporter genes depicted in E. Growth 'V' represents vegetative and 'R' represents respiratory conditions. Tub1p was used as internal loading control. Protein expression ratio between vegetative and respiratory conditions is shown in the bottom row. Error indicates standard deviation of three independent experiments. (G) The ratio of mitochondrial associated mRNA per cell of the reporter mRNAs in vegetative and respiratory conditions (n>34). Error bar represents s.e.m. Statistical significance was assessed by Mann–Whitney U-test (* P < 0.05; ns, no significant difference).

ized to the mitochondria under both conditions, showed no change in protein levels in respiratory conditions (Fig. 2A, B, C). This suggests that mRNA localization to mitochondria may drive increased protein production.

Given these results, we wanted to delve further into the mechanism of this varying localization and protein production. Even though the mitochondrial protein import machinery is well described, an ER-like signal recognition particle dependent mechanism of co-translational protein import has not been identified for the mitochondria (6, 7). However, a series of biochemistry and microscopy analysis showed that some nuclear encoded mitochondrial protein mRNAs are translated on the mitochondrial surface (2, 4, 8–12). We therefore investigated the effects of the MTS and of protein translation on mRNA association to mitochondria. We replaced the MTS of Tim50p with an ER-localization signal or introduced an ER-targeting signal at the N terminus of Tom22p (Fig. 2D) (13). Even though *TIM50* mRNA was associated with mitochondria, *ER-TIM50*, *TOM22*, and *ER-TOM22* mRNAs were not associated with mitochondria (Fig. 2D), indicating that the *TIM50* MTS is necessary to recruit mRNA to mitochondria. To further support the role of the MTS in mRNA localization, we tested whether reducing ribosome-nascent chain association by using the translation initiation inhibitor lactimidomycin (LTM) would affect mRNA localization (Fig. 2D). We found that *TIM50* mRNA in all conditions and *ATP3* mRNA in respiratory conditions decreased localization to the mitochondrial surface upon LTM addition, while *ATP3* mRNA in vegetative conditions showed only minimal changes in localization upon LTM addition (Fig. 2D). These results suggest that the actively translating ribosome drives mRNA localization to mitochondria through production of the nascent N-terminal MTS.

From our simulation we were able to recapitulate experimental results in which *TIM50* mRNA had higher affinity for the mitochondria than *ATP3* mRNA, making it less dependent on mitochondrial volume fraction. As the MTS was necessary for localization to the mitochondria, our initial hypothesis was that Tim50p MTS has a higher affinity for the mitochondria than the Atp3p MTS, causing the differences in mRNA affinities. To test this hypothesis, we designed chimeric GFP reporter genes wherein we swapped the MTS sequences between Tim50p and Atp3p under *TIM50* promoter control (Fig. 2E). Surprisingly, we found that the downstream coding sequence (CDS) was what differentiated *TIM50* from *ATP3* and not the MTS. When the reporter gene was tagged onto TIM50-CDS, it showed uniform protein pro-

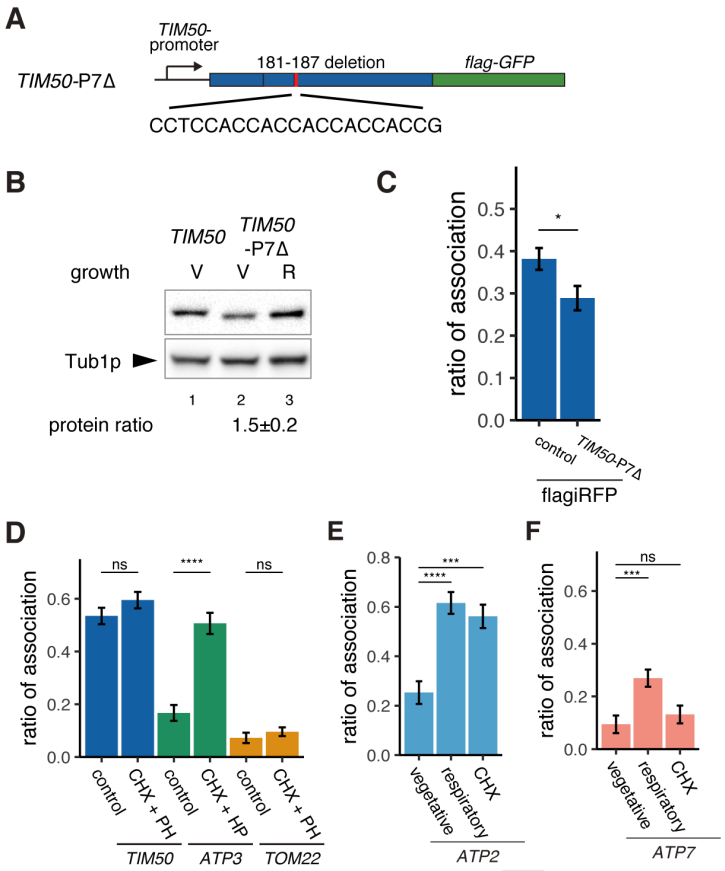

Fig. 3. Decreased translational elongation localizes mRNA to mitochondria. (A) Schematic of deletion of polyproline sequence from *TIM50-GFP* reporter gene. This construct is called *TIM50*-P7. (B) Protein expression from reporter genes *TIM50-GFP* and *TIM50*-P7. Growth 'V' and 'R' correspond to vegetative and respiratory conditions, respectively. Tub1p was used as internal loading control. Protein expression ratio between vegetative and respiratory conditions is shown in the bottom row. Error indicates standard deviation of three independent experiments. (C) The ratio of the mitochondrial associated mRNA per cell (n>20) of the reporter mRNAs in vegetative and respiratory conditions. Error bar represents s.e.m. Statistical significance was assessed by Mann–Whitney U-test (* $P < 0.05$; ns, no significant difference). (D) Translational inhibitor drugs alter the ratio of the mitochondrial associated mRNA per cell (n>43) of the strains in control (vegetative condition, Fig. 1C). CHX+PH indicates 100µg/mL cycloheximide and 200µg/mL 1,10-Phenanthroline for 10min. Error bar represents s.e.m. Statistical significance was assessed by Mann–Whitney U-test (**** $P < 0.0001$; ns, no significant difference). (E, F) The ratio of the mitochondrial associated mRNA per cell (n>16) of the different mRNA species in vegetative, respiratory, and CHX-treated conditions. Error bar represents s.e.m. Statistical significance was assessed by Mann–Whitney U-test (**** $P < 0.0001$; *** $P < 0.001$; ns, no significant difference).

duction in vegetative versus respiratory conditions, independent of which MTS was present (Fig. 2F lane 1 vs. 2 and lane 5 vs. 6). However, when the reporter gene was tagged onto ATP3-CDS, it showed decreased protein production in vegetative conditions (Fig. 2F lane 3 vs. 4 and lane 7 vs. 8). Similarly, the reporter genes that harbored the ATP3-CDS also showed decreased mitochondrial mRNA association ratios in vegetative conditions (Fig. 2G). These experiments suggest that the *TIM50* and *ATP3* MTS have similar affinities for the mitochondria, but that what drives the condition specific differences of mRNA localization and protein production between these mRNAs is encoded in the downstream CDS.

Our model proposes that the reason *ATP3* mRNA increases localization in respiratory conditions is that the increased mitochondrial volume fraction increases the probability that the nascent MTS will interact with the mitochondrial surface. If the *ATP3* and *TIM50* MTS have similar affinity for the mitochondria, we hypothesized the reason *TIM50* has higher mitochondrial association at lower mitochondrial volume fractions is because the downstream CDS increases the chance of association between mitochondria and MTS possibly by slowed translation elongation. Upon further examination we found that the *TIM50* downstream coding sequence has a 14 amino acid region approximately 60 amino acids downstream of the *TIM50* MTS that contains 10 proline residues, including 7 consecutive polyprolines. Polyproline stretches have been shown to mediate ribosome stalling and when we investigated a ribosome profiling data set we found that ribosomes accumulate at this polyproline stretch during vegetative conditions (Extended Data Fig. 5) (14). This suggests a possible mechanism, similar to what has been seen for SRP recognition, by which local slowdown of ribosomes increases the chance that the mitochondria will recognize the *TIM50* MTS and consequently promote its association with the mitochondrial surface (15). To test this, we deleted these polyproline residues and found this caused *TIM50* to be more sensitive to environmental conditions as it reduced the protein synthesis and mRNA localization of *TIM50* during vegetative conditions (Fig. 3A, B, C). In contrast, the *ATP3* coding sequence does not have any strong ribosome stalling sequence. This suggests that *ATP3* mRNA localization and protein synthesis are regulated solely in a mitochondrial volume fraction-dependent manner. If this is true, artifi-

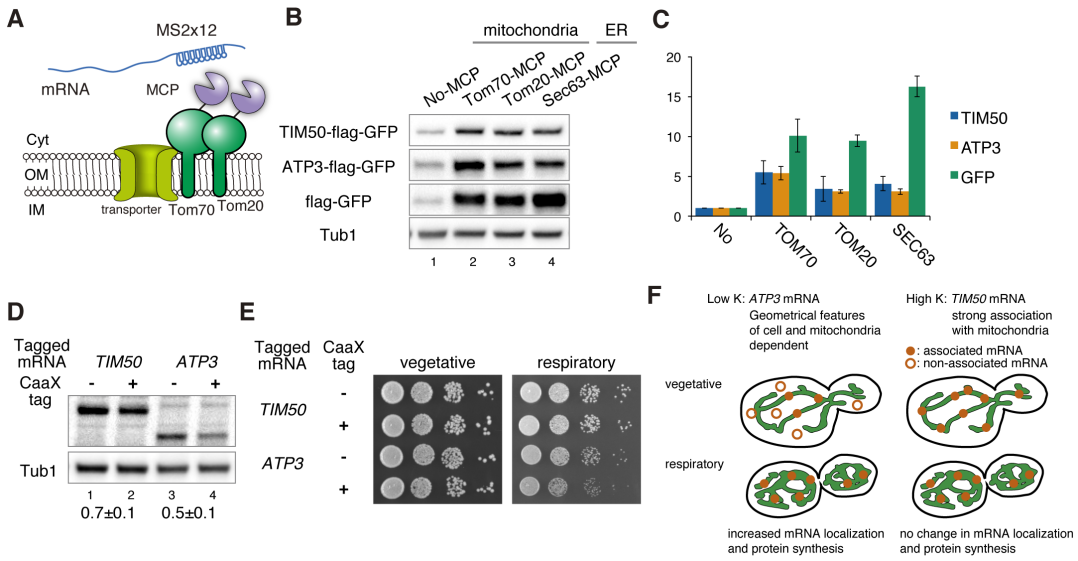

Fig. 4. mRNA localization to mitochondria enhances its translation. (A) Schematic of artificial mRNA tethering to mitochondria using MS2-MCP system. mRNA harboring a MS2 tandem sequence were tethered to mitochondria through C-terminus MCP tagged Tom70p or Tom20p. (B) Protein expression analysis of reporter mRNAs, which are tethered to mitochondria (lanes 2, 3) or ER (lane 4). Protein expression was analyzed using an anti-GFP antibody. Tub1p in the strain harbouring GFP-MS2 reporter genes was used as an internal loading control. (C) Quantification of B. Protein expression was normalized to the No-MCP strains. Error bar represents standard deviation of three independent experiments. (D) Protein expression analysis in anchored-away conditions. Protein expression levels in each strain in respiratory conditions were determined by Western blotting using flag-antibody. Protein expression ratio between strains with and without CaaX was shown at the bottom. Error indicates standard deviation of three independent experiments. (E) Growth assay for plasma membrane localized mRNA, which consists of an integrated MS2 sequence into the 3'-UTR of genomic DNA. *TIM50* and *ATP3* mRNAs were anchored away to the plasma membrane using CaaX-tag harbored MCP-GFP proteins. Cell growth was tested on YPAD (vegetative) and YPAGE (respiratory) conditions at 30℃ for 2 days and 3 days, respectively. (F) Mitochondria can coordinate gene expression during times of metabolic need via mitochondrial volume fraction-based control and simple chemical kinetics of nuclear-encoded mRNA localization bypassing nuclear gene regulation. mRNAs with low affinity for mitochondria localization are greatly affected by geometrical features of cells and mitochondrial volume fraction. When mitochondrial volume fraction is high in respiratory conditions, mRNA localization to mitochondria is increased and protein synthesis is induced by its localization. On the other hand, mRNAs with high affinity to mitochondria are always associated with mitochondria and thus not much affected by geometrical features.

cially slowing the ribosomes in vegetative conditions should drive *ATP3* mRNA to become mitochondrially localized. To test this hypothesis, we measured mitochondrial mRNA localization following the addition of cycloheximide (CHX), which slows translation elongation and stabilizes the mRNA-ribosome complex with the MTS, thereby giving it more time to associate with mitochondria (Fig. 3D). As our hypothesis predicted, we observed a three-fold increase in the association of *ATP3* mRNA with mitochondria during vegetative conditions but no increase in the case of *TOM22* mRNA (Fig. 3D). Interestingly, CHX treatment only slightly increased *TIM50* mRNA localization, potentially suggesting that most of these cytoplasmic mRNAs were already localized to the mitochondria.

A previous study found that 130 of 595 annotated nuclear-encoded mitochondrial mRNAs are sensitive to translation elongation rate and become localized to the mitochondrial surface upon cycloheximide treatment similar to *ATP3* (2). Interestingly, all of the ATP synthase subunits that are conserved from bacteria to eukaryotes are sensitive to cycloheximide, except for the ε subunit, *ATP16*, while all of the non-conserved subunits are insensitive to cycloheximide (Extended Data Sheet 1). We wondered if this sensitivity may be indicative of mRNAs that also switch their localization as the mitochondrial volume fraction increases during respiratory conditions (Extended Data Sheet 1). We found that *ATP2*, the conserved β subunit of the ATP synthase, was similar to *ATP3* in that it showed a large increase in localization upon a shift to respiratory conditions and was sensitive to cycloheximide (Fig. 3E). However, the non-conserved subunit, *ATP7*, behaved more like *TOM22*, where it was insensitive to cycloheximide and had a much smaller increase in mitochondrial localization in respiratory conditions than *ATP2* or *ATP3* (Fig. 3F).

These results suggest that mRNA localization to mitochondria may be a way to drive the coordinated increase in mitochondrial protein production observed in respiratory conditions. An alternative explanation is that increased translation drives more nascent protein production, which increases mRNA localization to the mitochondria. To directly test these two possibilities, we analyzed the effect of driving mRNA localization to mitochondria on protein expression. To accomplish this, we tethered reporter mRNAs to mitochondria by MS2 sequences. We inserted the MCP protein into the C-terminus of Tom20p and Tom70p, two well-characterized proteins on the outer mitochondrial membrane, and analyzed subsequent protein production (Fig. 4A). We found that tethering *TIM50-flag-GFP* and *ATP3-flag-GFP* mRNA to the mitochondria was sufficient to upregulate protein production. Surprisingly, protein production was increased independent of the mRNA harbouring an MTS. An mRNA that contained flag-GFP with no mitochondrial sequences also showed increased protein production (Fig. 4B, C). We then analyzed whether tethering to the ER might affect protein production by inserting the MCP protein into the C-terminus of Sec63p. We also saw increased protein pro-

duction when mRNA was tethered to the ER, suggesting that the surface of both of these organelles may harbour enhanced protein synthesis capacity. In addition to increased protein expression, we also observed increased mRNA levels when mRNAs were tethered to the mitochondria. However, the ratio of protein to mRNA was much higher (Extended Data Fig. 6, 7), suggesting that translational efficiency is increased on the mitochondrial surface. To test whether localization to the mitochondria is necessary for optimal protein production during respiratory conditions, we reduced the localization of endogenous *ATP3* and *TIM50* mRNA to mitochondria by directing those mRNAs to the plasma membrane via insertion of a CaaX-tag to the C termini of MCP-GFP proteins (16). This caused a decrease in protein levels of both ATP3-flag-GFP and TIM50-flag-GFP strains (Fig. 4D). We next investigated whether enhancing protein synthesis was essential for optimal cell growth. Cells in which *ATP3* mRNA was anchored to the plasma membrane and away from the mitochondria in respiratory conditions showed a growth defect whereas ER tethering of mRNAs, which does not impair protein synthesis, did not affect cell growth. (Fig. 4E, Extended Data Fig. 8). This suggests that localization of mRNA to mitochondria is important for optimal cell growth by driving enhanced protein synthesis during respiratory conditions.

Together, our results suggest the cell is able to use geometrical constraints that arise from increased mitochondrial volume fraction during respiratory conditions to drive localization of mRNAs to the mitochondrial surface (Fig 4F). Furthermore, we found that artificially tethering mRNA to organelles increased protein synthesis while anchoring mRNA away from the mitochondria reduced protein synthesis. These results strongly suggest that mRNA localization to the mitochondria is a way to control protein synthesis. We observed that the conserved subunits of ATP synthase were particularly sensitive to cycloheximide administration and that these subunits showed similar localization regulation patterns; this suggests a mechanism may have evolved that coordinates the expression and stoichiometry of vital subunits of this complex. However, how organelle localized mRNA can increase protein synthesis is still an open question. We consider the simplest explanation that there may be an increased density of ribosomes on the organelle surface since not only mitochondria but also ER tethered mRNAs increased protein production (Fig. 4B, C). It also might be true that translation initiation factors are highly phosphorylated around mitochondria since mitochondria produce high levels of ATP. An alternative, intriguing idea is that mitochondrial-localized ribosomes have specific modifications for enhancing translation (17). By using organelle volume fraction as a feedback mechanism to regulate organelle-specific gene expression through mRNA localization, this allows potential protein synthesis control without coordination with transcription of the nuclear genome. While we have found this gene expression control mechanism in yeast, we speculate higher eukaryotic cells could use organelle volume fraction dependent translation regulation as well. This could be especially important in neurons, which have high metabolic activity, but also must be able to regulate their gene expression in space and time while being remote from the cell body.

ACKNOWLEDGEMENTS

We thank members of the Zid laboratory as well as T. Endo, S. Iwasaki, E. Koslover, W. Wang and V. Bilanchone for helpful discussions and A. Subramaniam and S. Mukherji for feedback on the paper. Receipt of the MS2-tagging plasmids and yeast-optimized fluorophore plasmids from Dr. J. Gerst and Dr. K. Thorn is gratefully acknowledged. The authors also thank all members of the lab. We thank M. Zid, A. Guzikowski and V. Harjono for critically reading the manuscript. This work was supported in part by NSF grant MCB-1330451 and Ellison Medical Foundation (to S.M.R), startup funds from UCSD and from the National Institutes of Health R35GM128798 (to B.M.Z.), and NINDS P30NS047101 (to UCSD microscopy Core). T.T. acknowledges support from a Japan Society for the Promotion of Science (JSPS) for a research abroad fellowship and postdoctoral fellowship (18J00995), and Uehara Memorial Foundation for research abroad fellowship.

Bibliography

1. Mary T. Couvillion, Iliana C. Soto, Gergana Shipkovenska, and L. Stirling Churchman. Synchronized mitochondrial and cytosolic translation programs. *Nature*, 533(7604):499–503, 2016. ISSN 0028-0836. doi: 10.1038/nature18015.
2. C. C. Williams, C. H. Jan, and J. S. Weissman. Targeting and plasticity of mitochondrial proteins revealed by proximity-specific ribosome profiling. *Science*, 346(6210):748–751, 2014. ISSN 0036-8075. doi: 10.1126/science.1257522.
3. Mathilde Garcia, Thierry Delaveau, Sebastien Goussard, and Claude Jacq. Mitochondrial presequence and open reading frame mediate asymmetric localization of messenger RNA. *EMBO Reports*, 11(4):285–291, 2010. ISSN 1469221X. doi: 10.1038/embor.2010.17.
4. Noga Gadir, Liora Haim-Vilmovsky, Judith Kraut-Cohen, and Jeffrey E Gerst. Localization of mRNAs coding for mitochondrial proteins in the yeast Saccharomyces cerevisiae. *RNA (New York, N.Y.)*, 17:1551–1565, 2011. ISSN 1469-9001. doi: 10.1261/rna.2621111.
5. Alexander Egner, Stefan Jakobs, and Stefan W Hell. Fast 100-nm resolution three-dimensional microscope reveals structural plasticity of mitochondria in live yeast. *Proceedings of the National Academy of Sciences of the United States of America*, 99(6):3370–5, mar 2002. ISSN 0027-8424. doi: 10.1073/pnas.052545099.
6. A Golani-Armon and Y Arava. Localization of Nuclear-Encoded mRNAs to Mitochondria Outer Surface. *Biochemistry. Biokhimiia*, 81(10):1038–1043, 2016. ISSN 1608-3040. doi: 10.1134/S0006297916100023.
7. David W. Reid and Christopher V. Nicchitta. Diversity and selectivity in mRNA translation on the endoplasmic reticulum. *Nature Reviews Molecular Cell Biology*, 16(4):221–231, 2015. ISSN 14710080. doi: 10.1038/nrm3958.
8. Rod E. Kellems, Venita F. Allison, and Ronald A. Butow. Cytoplasmic Type 80 S Ribosomes Associated with Yeast Mitochondria. II. EVIDENCE FOR THE ASSOCIATION OF CYTOPLASMIC RIBOSOMES WITH THE OUTER MITOCHONDRIAL MEMBRANE IN SITU. *J. Biol. Chem.*, 249(10):3297–3303, may 1974.
9. Vicki AM Gold, Piotr Chroscicki, Piotr Bragoszewski, and Agnieszka Chacinska. Visualization of cytosolic ribosomes on the surface of mitochondria by electron cryo-tomography. *EMBO reports*, page e201744261, 2017. ISSN 1469-221X. doi: 10.15252/embr.201744261.
10. Philippe Marc, Antoine Margeot, Frederic Devaux, Corinne Blugeon, Marisol Corral-Debrinski, and Claude Jacq. Genome-wide analysis of mRNAs targeted to yeast mitochondria. *EMBO reports*, 3(2):159–64, feb 2002. ISSN 1469-221X. doi: 10.1093/embo-reports/kvf025.
11. Yann Saint-Georges, Mathilde Garcia, Thierry Delaveau, Laurent Jourdren, Stephane Le Crom, Sophie Lemoine, Veronique Tanty, Frederic Devaux, and Claude Jacq. Yeast mitochondrial biogenesis: a role for the PUF RNA-binding protein Puf3p in mRNA localization. *PloS one*, 3(6):e2293, jan 2008. ISSN 1932-6203. doi: 10.1371/journal.pone.0002293.
12. M Garcia, X Darzacq, T Delaveau, L Jourdren, R H Singer, and C Jacq. Mitochondria-associated yeast mRNAs and the biogenesis of molecular complexes. *Molecular biology of the cell*, 18(2):362–368, 2007. doi: 10.1091/mbc.E06.
13. B. Wu, C. Eliscovich, Y. J. Yoon, and R. H. Singer. Translation dynamics of single mRNAs in live cells and neurons. *Science*, 352(6292):1430–1435, 2016. ISSN 0036-8075. doi: 10.1126/science.aaf1084.
14. Brian M. Zid and Erin K. O'Shea. Promoter sequences direct cytoplasmic localization and translation of mRNAs during starvation in yeast. *Nature*, 514(7520):117–121, 2014. ISSN 14764687. doi: 10.1038/nature13578.
15. Justin W. Chartron, Katherine C.L. Hunt, and Judith Frydman. Cotranslational signal-independent SRP preloading during membrane targeting. *Nature*, 536(7615):224–228, 2016. ISSN 14764687. doi: 10.1038/nature19309.
16. Xiaowei Yan, Tim A. Hoek, Ronald D. Vale, and Marvin E. Tanenbaum. Dynamics of Translation of Single mRNA Molecules in Vivo. *Cell*, 165(4):976–989, 2016. ISSN 10974172. doi: 10.1016/j.cell.2016.04.034.
17. Shifeng Xue and Maria Barna. Specialized ribosomes: A new frontier in gene regulation and organismal biology. *Nature Reviews Molecular Cell Biology*, 13(6):355–369, 2012. ISSN 14710072. doi: 10.1038/nrm3359.